第478回電波研連F分科会資料
開催日：2003年10月23日

UWB Indoor Propagation Channel Measurement – Based on Deterministic Approach –

Katsuyuki Haneda, Jun-ichi Takada
Department of International Development Engineering
Tokyo Institute of Technology
2–12–1, O-okayama, Meguro-ku, Tokyo, Japan
Telephone, FAX: +81–3–5734–3288
Email: haneda@ap.ide.titech.ac.jp

***Abstract*— In this paper, a new Ultra Wideband (UWB) channel estimation algorithm, UWB-SAGE (Space Alternating Generalized Expectation Maximization) is proposed. In the algorithm, a novel UWB signal model which is an extention of the conventional wideband signal model is employed in order to estimate the UWB channel with SAGE algorithm. The algorithm divides the measured data into individual ray paths and estimates the directions of arrival, propagation time, and the variation of the amplitude and phase during the propagation for each signal. The measurement campaign in indoor environment was conducted and it was shown that the algorithm could correctly extract the inherent propagation phenomena of the channel. The estimation result can be very useful for the design and analysis of UWB communication system, especially for the evaluation of waveform distortion and multipath effect.**

I. INTRODUCTION

Recent communication networks are required higher data rate than ever and the UWB communication system has drawn a lot of interests as a promising scheme to realize this requirement. In order to construct an efficient UWB system, it is required to investigate the propagation channel where the system is to be implemented . Characterization of the channel has been done by estimating the directions of arrival (DOAs) and directions of departure (DODs) and the times of arrival (TOAs) of the waves from Tx to Rx. Channel modelling and clusterization of the potential scatterers are also important.

There have already been constructed theoretical and experimental schemes of channel sounding for wideband channels[1], [2]. The measurement is often conducted by using PN sequences and data processing is done in the frequency domain. In the modelling of collected data, it is required that the variation of transfer function within the considered bandwidth B and antenna aperture A is sufficiently small, namely, a condition

$$B\frac{A}{c} \ll 1 \tag{1}$$

must be held where c is light velocity. However, this condition is not satisfied in UWB systems.

For UWB channel estimation, the use of Sensor-CLEAN algorithm has been proposed [3], [4]. This algorithm estimates not only DOAs and TOAs but also incident waveforms, thus sequential data in time domain is necessary.

In this paper, we propose a frequency domain channel sounding scheme for UWB system, namely Ultra-Wide Bandwidth Space Alternating Generalized Expectation Maximization (UWB-SAGE) algorithm. In the algorithm, a novel UWB signal model which is an extention of the conventional wideband signal model is employed in order to estimate the UWB channel with SAGE algorithm. The SAGE algorithm has been adopted for wideband channel estimation [5], [6]. In UWB-SAGE, waveform estimation is not necessary because the algorithm assumes the transmit waveforms to be *known* in the receiver side and employs frequency domain processing. The frequency domain measurement is easily implemented with vector network analyzer and spatially scanning antenna [7] thus the algorithm is applicable for real environment estimation. Note that the UWB communication is deployed only for short range environment so that it is enough to consider the network analyzer based system.

II. PATH MODEL

In the ray based propagation model which is applicable for high frequency waves (also for UWB communication), it can be defined that one propagation path has DOD, DOA and TOA that does not depend on frequency, but has a frequency dependent complex gain. Herein a single directional measurement model is considered i.e., DOD is not estimated, hence the transfer function of one ray path $y_l(f, \phi_l, \theta_l, \tau_l)$ is expressed as

$$y_l(f, \phi_l, \theta_l, \tau_l) = \alpha_l(f, \tau_l) r_l(f) D(f, \phi_l, \theta_l) \tag{2}$$

where

- τ_l : propagation time,
- ϕ_l : arrival azimuth angle,
- θ_l : arrival elevation angle,
- $\alpha_l(f, \tau_l)$: complex gain of the spatial propagation,
- $r_l(f)$: scattering loss,
- $D(f, \phi_l, \theta_l)$: radiation pattern of Rx antenna for a single polarization.

Note that the gain of Tx antenna can not be modeled in Eq. (2). Therefore, this effect is included in $r_l(f)$ in this model. $\alpha(f, \tau)$ can be expressed as the extension of Friis'

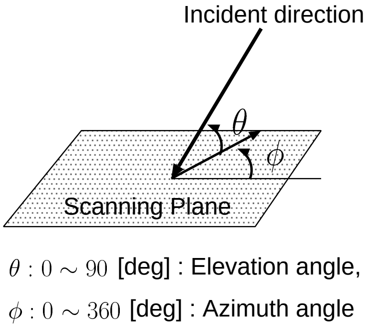

Fig. 1. Definition of Angles at Rx

Transmission Formula,

$$\alpha_l(f,\tau_l) = \frac{1}{4\pi\tau_l f}\exp\left(-\mathrm{j}2\pi\tau_l f\right). \tag{3}$$

III. UWB-SAGE ALGORITHM

UWB-SAGE algorithm is based on the Maximum Likelihood Estimation (MLE) and has a high resolution in separating the incident waves.

A. The Data Model

Suppose that UWB channel can be expressed as the superposition of I subbands where the scattering loss and the antenna directivity within each subband is assumed to be constant. When we focus on the ith subband whose center frequency is $f_{\mathrm{c}i}$ $(1 \leq i \leq I)$, we can formulate a model of a measured transfer function. Suppose there are L waves incident to uniform rectangular array (URA) in horizontal plane which has equally spaced $M_1,\ M_2$ antenna elements in azimuth and elevation directions. The azimuth and elevation angles are defined as Fig. 1. The element spacings are Δ_x and Δ_y, respectively. By performing M_3 frequency sweeping with sampling interval Δ_f at center frequency $f_{\mathrm{c}i}$, the measured transfer function y_{k_1,k_2,k_3} is denoted as Eq. (4),

$$\begin{aligned} y_{k_1,k_2,k_3} \;=\; & \sum_{l=1}^{L}\left[\alpha_l(f_{\mathrm{c}i},\tau_l)r_l(f_{\mathrm{c}i})D(f_{\mathrm{c}i},\phi_l,\theta_l)\prod_{r=1}^{3}e^{\mathrm{j}k_r\mu_{l,i}^{(r)}}\right] \\ & +n_{k_1,k_2,k_3}. \end{aligned} \tag{4}$$

where $0 \leq k_r \leq M_r-1$ $(1 \leq r \leq 3)$ indicates a index number of each sampling domain. n_{k_1,k_2,k_3} is white gaussian noise of zero mean. $\mu_{l,i}^{(r)}$ is expressed as

$$\mu_{l,i}^{(1)} = \frac{2\pi f_{\mathrm{c}i}}{c}\Delta_x \sin\phi_l\cos\theta_l, \tag{5}$$

$$\mu_{l,i}^{(2)} = \frac{2\pi f_{\mathrm{c}i}}{c}\Delta_y \cos\phi_l\cos\theta_l, \tag{6}$$

$$\mu_{l,i}^{(3)} = 2\pi\Delta_f\tau_l. \tag{7}$$

Plane wave approximation of the incident wave is used in this formulation.

For simplicity, we vectorize the data defined in Eq. (4) as

$$\begin{aligned} \mathbf{y}_i \;=\; & [y_{1,1,1,i}\ y_{2,1,1,i}\ \cdots\ y_{M_1,1,1,i}\ y_{1,2,1,i}\cdots \\ & y_{M_1,M_2,1,i}\ y_{1,1,2,i}\ \cdots\ y_{M_1,M_2,M_3,i}]^T \in C^M \\ =\; & \mathbf{A}_i\mathbf{s}_i + \mathbf{n}_i, \end{aligned} \tag{8}$$

where $M = M_1M_2M_3$ and $\mathbf{n}_i$ is noise vector. $\mathbf{s}_i$ denotes a transfer function vector that is composed of propagation and antenna characteristics of each wave. Namely,

$$\begin{aligned} \mathbf{s}_i \;=\; & [s_{1,i}\ s_{2,i}\ \cdots\ s_{L,i}]^T \\ =\; & [\alpha_1(f_{\mathrm{c}i},\tau_1)r_1(f_{\mathrm{c}i})D(f_{\mathrm{c}i},\phi_1,\theta_1),\ \cdots \\ & \alpha_L(f_{\mathrm{c}i},\tau_L)r_L(f_{\mathrm{c}i})D(f_{\mathrm{c}i},\phi_L,\theta_L)]^T \in C^L. \end{aligned} \tag{9}$$

The multi-dimensional mode matrices $\mathbf{A}_i \in C^{M\times L}$ is expressed as Eq. (10),

$$\mathbf{A}_i = \mathbf{A}_i(\mu_i^{(3)}) \diamond \mathbf{A}_i(\mu_i^{(2)}) \diamond \mathbf{A}_i(\mu_i^{(1)}), \tag{10}$$

where

$$\mathbf{A}_i(\mu_i^{(r)}) = \left[\mathbf{a}_i(\mu_{1,i}^{(r)})\ \cdots\ \mathbf{a}_i(\mu_{L,i}^{(r)})\right]^T, \tag{11}$$

$$\mathbf{a}_i(\mu_{l,i}^{(r)}) = \left[1\ e^{\mathrm{j}\mu_{l,i}^{(r)}}\ \cdots\ e^{\mathrm{j}(M_r-1)\mu_{l,i}^{(r)}}\right]^T, \tag{12}$$

and $\diamond$ denotes the Kronecker product of each column of the matrices.

The UWB channel model can be derived as a simple I superposition of this subband model.

B. SAGE Algorithm

MLE estimates a component that maximize the likelihood function, which is the probability of observing the measured data by assuming that the data follows a certain distribution. In the considered signal model, the received signal is perturbed by gaussian noise. Therefore, the probability of generating the measured data vector $\mathbf{y}_i$ from signal component vector $\boldsymbol{\mu}_i$, $p(\mathbf{y}_i|\boldsymbol{\mu}_i)$ is

$$\begin{aligned} p(\mathbf{y}_i|\boldsymbol{\mu}_i) \;=\; & \prod_{k_1=1}^{M_1}\prod_{k_2=1}^{M_2}\prod_{k_3=1}^{M_3}\left(\frac{1}{\pi\sigma}\times\right. \\ & \left.\exp\left[-\frac{|y_{k_1,k_2,k_3,i}-\mu_{k_1,k_2,k_3,i}|^2}{\sigma^2}\right]\right) \end{aligned} \tag{13}$$

where the noise is assumed to be independent and identically distributed.

By taking the logarithm, the maximum likelihood condition is expressed as the following minimization problem,

$$\arg\max_{\boldsymbol{\mu}} \ln p(\mathbf{y}_i|\boldsymbol{\mu}) = \frac{1}{\sigma^2}\arg\min_{[\phi_l,\theta_l,\tau_l,s_l]_{l=1}^{L}} ||\mathbf{y}_i - \mathbf{A}_i\mathbf{s}_i||^2. \tag{14}$$

The required search in Eq. (14) is a simultaneous $4L$ dimensional one.

To reduce the computationally prohibitive multidimensional simultaneous search, the Expectation-Maximization (EM) algorithm is introduced [8]. This estimates the complete data $\mathbf{x}_{l,i}$ from the incomplete data $\mathbf{y}_i$ as Eq. (15).

$$\mathbf{x}_{l,i} = \mathbf{a}_{l,i}s_{l,i} + \beta_{l,i}(\mathbf{y}_i - \mathbf{A}_i\mathbf{s}_i) \tag{15}$$

Herein the nature of the additive white gaussian noise is considered in the derivation and the initial values of the parameters are needed. $\beta_{l,i}$ is a positive number which has a constraint $\sum_{l=1}^{L} \beta_{l,i} = 1$ but is practically set to 1. This makes us possible to maximize the conditional Fisher information of complete data $\mathbf{x}_{l,i}$[6]. In our case, incomplete data means the measured data and complete data corresponds to the data of each incident waves which are not directly measured in the experiment. The modified log-likelihood function for complete data is analogous to Eq. (14),

$$\arg\max_{\boldsymbol{\mu}} p(\mathbf{x}_{l,i}|\boldsymbol{\mu}) = \arg\min_{[\phi,\theta,\tau,s]} ||\mathbf{x}_{l,i} - \mathbf{a}_i s_i||^2. \tag{16}$$

This means that the simultaneous search dimension is reduced to 4. We can see that the search estimates the parameters of the waves which extract the largest power from the complete data. Thus, we can rewrite this minimization procedure in the following 3-dimensional simultaneous search.

$$(\hat{\phi}_l, \hat{\theta}_l, \hat{\tau}_l) = \arg\max_{[\phi,\theta,\tau]} \mid z(\phi, \theta, \tau, \mathbf{x}_{l,i}) \mid \tag{17}$$

The cost function $z(\phi, \theta, \tau, \mathbf{x}_{l,i})$ is denoted as

$$z(\phi, \theta, \tau, \mathbf{x}_{l,i}) = E[\mathbf{a}_i^H \mathbf{x}_{l,i}]. \tag{18}$$

This is equivalent to finding the matched filter for a certain incident wave. The complex transfer function of the wave $s_{l,i}$ is derived from the estimated parameters as,

$$s_{l,i} = \frac{z(\hat{\phi}_l, \hat{\theta}_l, \hat{\tau}_l, \mathbf{x}_{l,i})}{M}, \tag{19}$$

and the path gain $P_{l,i} = |s_{l,i}|^2$ is obtained.

SAGE algorithm divides the whole search space of EM algorithm into hidden data spaces. In our case, the search is carried out sequentially in the following order,

$$\hat{\phi}_l = \arg\max_{\phi} \mid z(\phi, \theta_l, \tau_l, \mathbf{x}_{l,i}) \mid, \tag{20}$$

$$\hat{\theta}_l = \arg\max_{\theta} \mid z(\hat{\phi}_l, \theta, \tau_l, \mathbf{x}_{l,i}) \mid, \tag{21}$$

$$\hat{\tau}_l = \arg\max_{\tau} \mid z(\hat{\phi}_l, \hat{\theta}_l, \tau, \mathbf{x}_{l,i}) \mid . \tag{22}$$

In this way, we can obtain updated estimates of parameters from the old ones. This process is repeated until the likelihood reaches a certain maximum value or the estimated parameters converge on some fixed value.

C. UWB-SAGE Algorithm

As explained in section III-A, UWB channel can be expressed as a set of subbands. Therefore, in the UWB channel estimation, the cost function to be maximized $z(\phi, \theta, \tau, \{\mathbf{x}_{l,i}\}_{i=1}^{I})$ is a simple summation of modified log-likelihood of each subband as Eq. (23).

$$z(\phi, \theta, \tau, \{\mathbf{x}_{l,i}\}_{i=1}^{I}) = \sum_{i=1}^{I} \left| E[\mathbf{a}_i^H \mathbf{x}_{l,i}] \right| \tag{23}$$

In the use of SAGE algorithm, SIC (Successive Interference Cancellation) type procedure is preferable when the number of samples is sufficiently large [7], [9]. An example of the search procedure is depicted in Fig. 2. This scheme is a combination of local search based on SAGE algorithm and global mesh search based on EM algorithm. In global mesh search, we aim at the region which may include a maximum point of the cost function. After that, local search is carried out inside the selected region to find an accurate peak. The process is repeated until the number of detected paths reaches the predefined number of waves or the detected path level falls below the noise floor level. The transfer function of ith subband channel is obtained from Eq. (19).

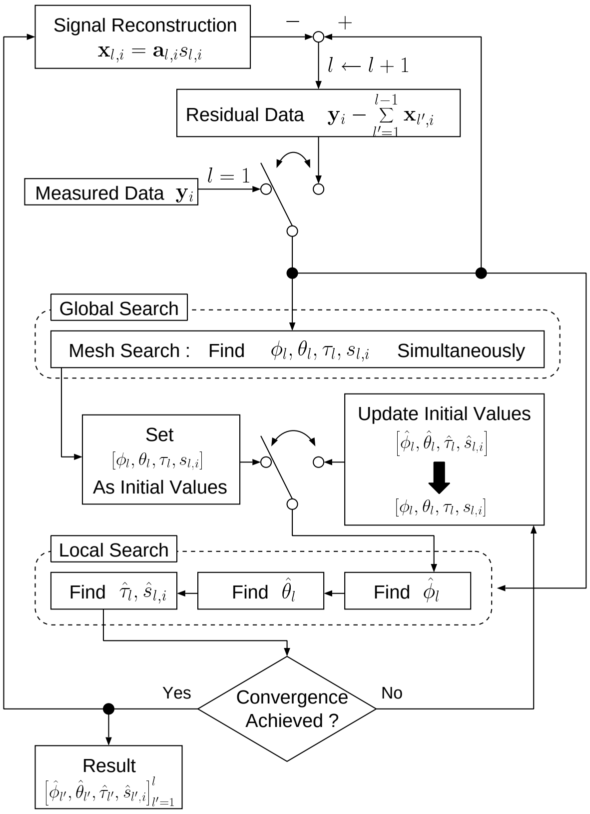

Fig. 2. Flow chart of the SAGE algorithm of SIC type for each subband [9].

It should be pointed out that the system parameters to be optimized in the estimation are the following two, which must be adjusted within the criteria of Eq. (1):

1) Sampling interval of frequency domain Δ_f.
   Δ_f gives the upper bound of arrival time without the appearance of aliasing, $\tau_{\max} = \frac{1}{\Delta_f}$.
2) The number of samples in spatial domain M_1, M_2 and in frequency domain $M_3 I$.
   These parameters decide the basic resolution of the algorithm.

IV. UWB CHANNEL MEASUREMENT

A. Measurement System and Environment

With the UWB-SAGE algorithm and measurement system proposed in [7], we estimated typical indoor channel with

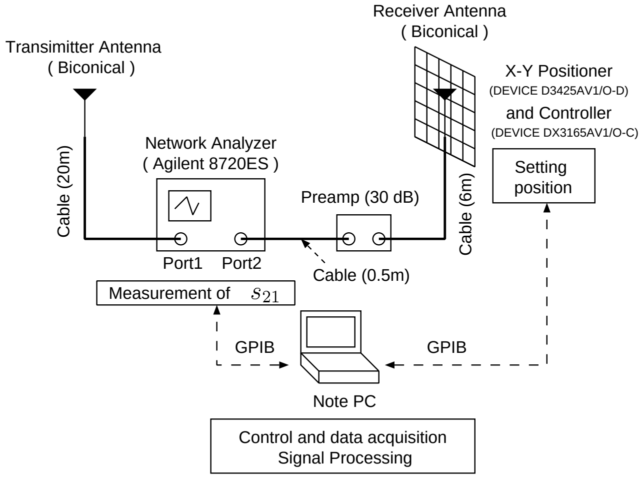

Fig. 3. UWB channel measurement system.

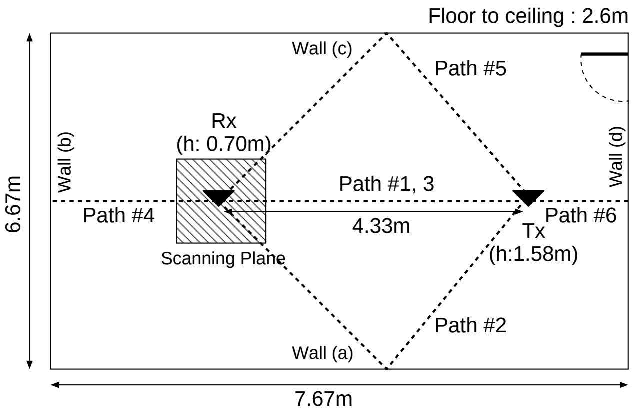

Fig. 4. Floor plan of the measurement environment and result of path identification.

UWB signal in order to assess the validity. Figure 3 is the architecture of the measurement system. The system measures the transfer function by Vector Network Analyzer (VNA) and the synthesyzed antenna aperture is achieved with one element antenna and spatial scanner.

The floor plan of the measurement environment is depicted in Fig.4. The Tx and Rx antennas are set in the same room with different height. The size of the room is about 6.7×7.7 $[\mathrm{m}^2]$ and are typical small conference room. There is almost no objects in the room except for the measurement equipment. During the experiment, the door was closed so that the channel was considered to be time invariant. The specifications of the measurement and UWB-SAGE algorithm implementation are listed in Table I. Note that the back-to-back calibration is a simplified procedure which removes the mismatch loss occured between cables and antennas. In the case of executing this procedure, it should be satisfied that only the direct path exists. Therefore, in the on-site calibration as our experiment, we used the electromagnetic absorber so as to isolate the Tx and Rx antennas from objects surrounded.

TABLE I

SPECIFICATIONS OF THE MEASUREMENT

Bandwidth considered	3.1 [GHz] $\sim$ 10.6 [GHz][10]
The number of samples in frequency domain	751 points ($\Delta_f = 10$ [MHz]).
Bandwidth of each subband	800 [MHz]
The number of samples in spatial domain	In horizontal plane, 10×10 points of rectangular array configuration whose intervals are 4.8 [cm](less than half wavelength in 3.1 [GHz])
Estimated components	Azimuth ϕ, elevation θ, propagation time τ and variation of spectrum in terms of phase and gain.
Antennas	Biconical antennas for Tx and Rx.
IF Bandwidth	100 [Hz].
Polarization of the wave	Vertical–Vertical.
Noise level of network analyzer	-98 [dBm].
Resolution of UWB-SAGE algorithm	10 [deg] for azimuth or elevation, 0.2 [ns] in time domain.
Calibration	Back-to-back, the distance between Tx and Rx is 0.7 [m].

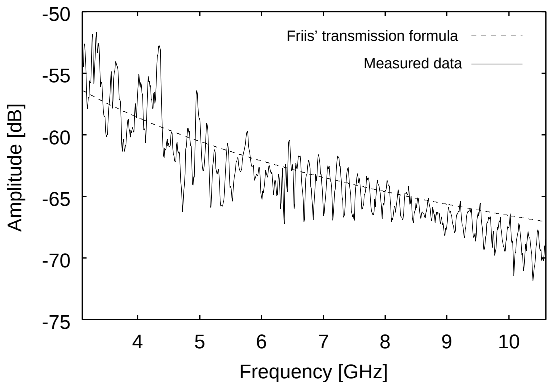

Fig. 5. Measured power spectrum and the Friis's free space transmission formula.

B. Results

Figure 5 is the averaged power spectrum obtained from VNA. The free space gain of direct wave derived from Friis' transmission formula [11] is also shown. They have small difference and it is assumed that the direct component is dominant in this line-of-sight environment. The fluctuation of the measured power spectrum is due to the multipath effect.

The results of parameters estimation with UWB-SAGE algorithm is shown in Table II. There are 6 waves detected including direct path and reflected rays from each side of the walls. In the table, parameters derived from geometical optics method (GO) are shown as well and they agree well with the estimated ones. This means that all the waves are almost identical to the specular reflected paths. For all the paths, we can see some deviation between the estimated result and the one derived by the GO. In angle domain, this kind of error

TABLE II

Result of parameters estimation by UWB-SAGE algorithm

Path identification	Azimuth [deg]	Elevation [deg]	Delay [ns]
#1 Direct wave	359.30 (0.00)	13.80 (11.49)	15.30 (14.73)
#2 Wall(a) rflct.	303.70 (302.04)	13.80 (6.15)	29.03 (27.37)
#3 Ceiling rflct.	358.90 (0.00)	29.90 (34.00)	18.63 (17.40)
#4 Wall(b) rflct.	180.90 (180.00)	13.40 (5.25)	34.70 (32.03)
#5 Wall(c) rflct.	61.60 (56.00)	15.40 (6.48)	29.86 (25.98)
#6 Wall(d) rflct.	359.70 (0.00)	11.3 (8.07)	21.49 (20.91)

is due to the worse accuracy of endfire direction estimation. On the other hand, phase characteristics of the antennas could cause a bias on the delay estimation, although the effect is not significant.

The estimated gain and phase of direct path are depicted in Fig. 6. The phase shown in the figure indicates the deviation from the free space phase variation, namely in this case, the phase rotation at antennas. For the reflected waves, the phase component obtained in the estimation includes both antennas and reflection (scattering) phase characteristics.

V. Conclusion

We proposed an algorithm which estimates the UWB propagation channel in a deterministic way, named UWB-SAGE. This algorithm employs the novel UWB signal model which is an extension of conventional wideband signal model and conducts a frequency domain processing, therefore the estimation of time domain waveforms is not required. The indoor channel measurement suggested that the algorithm could correctly separate the incident waves and evaluate the parameters of each wave.

In the processing of UWB-SAGE, antenna directivity is regarded as isotropic because of the difficulty of embedding them into multi-dimensional mode matrix $\mathbf{A}_i$ in Eq. (8). Therefore, the estimation results include both characteristics of antenna and propagation. For the spectrum, propagation characteristics can be extracted from the estimated result by deconvoluting the effect of antenna directivity and its frequency dependence.

We must assess our algorithm in several aspect, for example, experimental velification of the resolution. The behavior of the algorithm for the estimation of waves whose delays and angles are much closer compared to the resolution is also of the interest. At the same time, several measurements not only in LOS but also in NLOS environments are needed for the aim of UWB channel modelling.

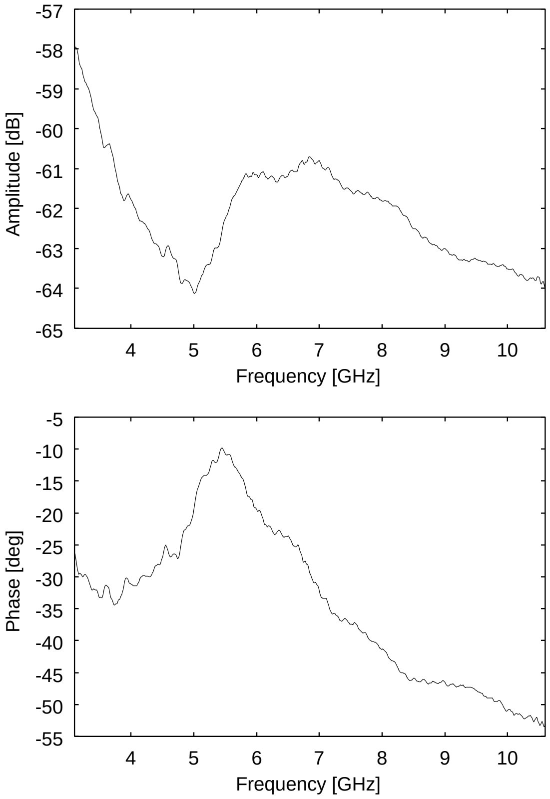

Fig. 6. Estimated amplitude and phase of direct wave.

References

[1] K. Kalliola, H. Laitinen, L. I. Vaskelainen and P. Vainikainen, "Real-time 3D spatial-temporal dual-polarized measurement of wideband radio channel at mobile station", *IEEE Trans. Instrum. and Meas.*, Vol. 49, No. 2, pp. 439–448, Apr. 2000.

[2] R. S. Thomä, D. Hampicke, A. Richter, G. Somerkorn, A. Schneider, U. Trautwein, and W. Wirnitzer, "Identification of time-variant directional mobile radio channels", *IEEE Trans. Instrum. and Meas.*, Vol. 49, No. 2, pp. 357–364, Apr. 2000.

[3] R. J. Cramer, R. A. Scholtz, M. Z. Win, "Evaluation of an ultra-wide-band propagation channel", *IEEE Trans. Antennas Propagat.*, Vol. 50, No. 5, pp. 561–570, May 2002.

[4] A. S. Y. Poon and M. Ho, "Indoor multiple antenna channel characterization from 2 to 8 GHz" *2003 IEEE Int. Conf. on Commun.*, GC27-3, Anchorage, AK., May 2003.

[5] J. A. Fessler and A. O. Hero, "Space-alternating generalized expectation-maximization algorithm", *IEEE Trans. Signal Processing*, Vol. 42, pp. 2664–2677, Oct. 1994.

[6] B. H. Fleury, M. Tschudin, R. Heddergott, D. Dahlhaus, and K. I. Pedersen. "Channel parameter estimation in mobile radio environments using the SAGE algorithm", *IEEE J. Select. Areas Commun.*, Vol. 17, No. 3, pp. 434–449, Mar. 1999.

[7] K. Haneda and J. Takada, "High-resolution estimation of NLOS indoor MIMO channel with network analyzer based system", in *Proc. Personal Indoor and Mobile Radio Communication 2003 (PIMRC2003)*, Beijing, China, pp. 675–679, Sept. 2003.

[8] A. P. Dempster, N. M. Laird, and D. B. Rubin, "Maximum likelihood from incomplete data via the EM algorithm", *J. Royal Statist. Soc., Ser.B*, Vol. 39, No. 1, pp. 1–38, 1977.

[9] B. H. Fleury, X. Yin, K. G. Rohbrandt, P. Jourdan, and A. Stucki, "Performance of a high-resolution scheme for joint estimation of delay and bidirection dispersion in the radio channel", in *Proc. IEEE 55th Veicular Technology Conference (VTC 2002/Spring)*, May 2002.

[10] Federal Communications Commission, "Revision of part 15 of the commission's rules regarding ultra-wideband transmission systems", *First Report and Order*, FCC 02–48, Apr. 2002.

[11] H. T. Friis, "A note on a simple transmission formula", in *Proc. IRE*, Vol. 34, No. 5, pp. 254–256, May 1946.